Supporting Information for "Seasonal freeze-thaw cycles and permafrost degradation on Mt. Zugspitze (German/Austrian Alps) revealed by single-station seismic monitoring"

Fabian Lindner[1], Joachim Wassermann[1], Heiner Igel[1]

[1]Department of Earth and Environmental Sciences, LMU Munich, Theresienstraße 41, 80333, Munich, Germany

Contents of this file

Text S1: Moving reference approach

To extract travel time shifts, time-lapse cross-correlations are compared to a reference cross-correlation. If travel time shifts change smoothly but reach large values relative to the reference period such that cycle skipping occurs, one may compare cross-correlations from adjacent dates (e.g. this week versus last week), assuming small velocity changes between the dates. This is relevant for permafrost monitoring, as thaw and refreeze can be

———

June 2, 2021, 3:58pm

associated with such strong velocity changes, that the measurement of travel time shifts is affected by cycle skipping (James et al., 2017, 2019). We therefore also determine travel time shifts using a moving reference similar as in James et al. (2017), in addition to the fixed reference approach. Here, we are dealing with smooth seasonal velocity changes, which we determine in a first step with a moving approach for 2016 (no gaps and no changes in instrumentation): For each 15 d moving stack in 2016, we determine $\delta t(t, f)$ relative to the previous, neighbouring 15 d stack that is not overlapping with the current stack (e.g. 2016-02-01 serves as reference for 2016-02-16). In case the reference dates back to 2015, we take 2016-01-01 as reference (e.g. 2016-01-01 serves as reference for 2016-01-05). To obtain meaningful time series, we then accumulate the travel time shifts from neighbouring 15 d stacks, e.g. for 2016-02-26 we sum up the values obtained for 2016-01-12 (relative to 2016-01-01), 2016-01-27, and 2016-02-11. Thereby, we strictly speaking end up with 15 time series relative to 2016-01-01, together building the seasonal cycle for 2016. In the second step, we determine all deviations from this cycle: for each 15 d stack outside 2016, we calculate $\delta t(t, f)$ relative to the respective date in 2016, e.g. for 2007-08-19 we use 2016-08-19 as reference, and sum up the travel time shifts of both dates.

The described procedure assumes a periodic velocity change cycle with similar velocity changes at the same date at different years. In summary, we first determine the variations in 2016 and subsequently the changes relative to 2016, hence cycle skipping should be eliminated for smooth travel time changes with a periodicity of one year. This strategy further keeps the number of summations and thus the error propagation at a moderate

level compared to using a moving reference for the complete data set of 15 years. Furthermore, the latter can hardly be applied, as data gaps prevent the continuous travel time tracking, resulting in erroneous offsets.

Text S2: Velocity change results obtained from different approaches

In most applications, $-\delta t/t$ is obtained from linear regression using travel time shifts δt at different lag times t and the results are typically interpreted as velocity change dv/v, which is exact in the case of a bulk velocity change affecting the whole medium of consideration. In this study, we used only specific parts of the cross-correlation showing high 365.25 d periodicity and determined $-\delta t/t$ as the median from individual $-\delta t/t$ curves for each frequency bin. In this section, we examine different scenarios for the $-\delta t/t$ extraction including linear regression for each frequency bin and the classical moving-window cross-spectral (MWCS) technique. To facilitate the comparison of the different approaches, we determine the key quantities, i.e. the seasonal velocity change and the long-term velocity change, by fitting a model consisting of the superposition of a sinusoid and a linear trend to the $-\delta t/t$ time series, i.e.

$$\Delta_m \;=\; c_1 \,\cos(2\pi f_{yr} t_{UTC}) \;+\; c_2 \,\sin(2\pi f_{yr} t_{UTC}) \;+\; c_3 \,t_{UTC} \;+\; c_4, \tag{1}$$

where f_{yr} is the frequency of one year, i.e. the inverse of 365.25 d, and t_{UTC} refers to the absolute time. Employing linear least squares to fit the model to the data, we obtain the constants c_1 to c_4, which we use to calculate the seasonal peak-to-peak velocity change given by $2\sqrt{c_1^2 + c_2^2}$. In addition, c_3 yields the slope, i.e. the linear trend. Furthermore,

one may calculate the phase of the sinusoid given by $arctan2(c_2/c_1)$, which can be used to determine the timing of the seasonal maxima and minima of the sinusoid.

Because component NZ yields the most consistent results between 2 and 8 Hz for both the fixed and the moving reference (smaller standard deviation than EN and EZ components), we focus the comparison on this component and frequency range. Fig. S1a (black line) shows the NZ $-\delta t/t$ curve from Fig. 3d (main manuscript) relative to the fixed reference, i.e. the median $-\delta t/t$ curve for each frequency bin considering only those that show a normalized Lomb-Scargle amplitude of at least 0.15 and subsequently averaged over 2-8 Hz. Furthermore, Fig. S1a shows the model fit (eq. 1) to this curve (orange dashed line). The corresponding peak-to-peak amplitude of seasonal velocity changes exceeds 3% and the velocity decreases on average by about 0.11 %/yr (scenario 1 in Fig. S1b). Similar results are obtained when using the moving reference (3.7% peak-to-peak and -0.08 %/yr, scenario 2). Next, we also consider the common approach of using a linear regression (here without applying weights) at each time step to determine a $-\delta t/t$ time series for each frequency bin (using again one and 15 periods as lag time limits). We use the fixed reference and consider only those lag times with $A_{LS}(365.25d) \geq 0.15$ (scenario 3) and regardless of $A_{LS}(365.25d)$ (i.e. using all δt values in the considered lag range, scenario 4). For the 2-8 Hz averaged results, we obtain peak-to-peak amplitudes of 2.5 % and 0.9 % (scenarios 3 and 4, respectively) and long-term velocity decreases of -0.085 %/yr and -0.04%/yr. Finally, we consider the $-\delta t/t$ curve obtained from the widely used MWCS analysis in the lag and frequency range of 0.5-4 s and 2-8 Hz, respectively (scenario 5). Within the lag window, we use a moving window of 0.75 s width with overlap of 0.5 s to

determine the frequency-averaged travel time shifts as a function of lag time, which we subsequently use in a linear regression to determine $-\delta t/t$. The resulting velocity changes and the corresponding model fit are shown in Fig. S1a (grey and red line, respectively). Also here, we find a seasonal velocity variation with peak-to-peak amplitude of 1 % and a velocity decrease of -0.01 %/yr. However, we note that when using MWCS, only component NZ shows clear seasonal velocity variations. With regard to the phase of the seasonal velocity changes, all scenarios yield delays ranging between 50 and 60 d, meaning that the annual maximum of the sinusoid model is reached in late February to early March. While all approaches yield a similar velocity change pattern, the velocity change amplitudes are dependent on the processing and the selected coda wave windows.

References

James, S., Knox, H., Abbott, R., Panning, M., & Screaton, E. (2019). Insights into permafrost and seasonal active-layer dynamics from ambient seismic noise monitoring. *Journal of Geophysical Research: Earth Surface*, *124*(7), 1798–1816.

James, S., Knox, H., Abbott, R., & Screaton, E. (2017). Improved moving window cross-spectral analysis for resolving large temporal seismic velocity changes in permafrost. *Geophysical Research Letters*, *44*(9), 4018–4026.

Lecocq, T., Caudron, C., & Brenguier, F. (2014). Msnoise, a python package for monitoring seismic velocity changes using ambient seismic noise. *Seismological Research Letters*, *85*(3), 715–726.
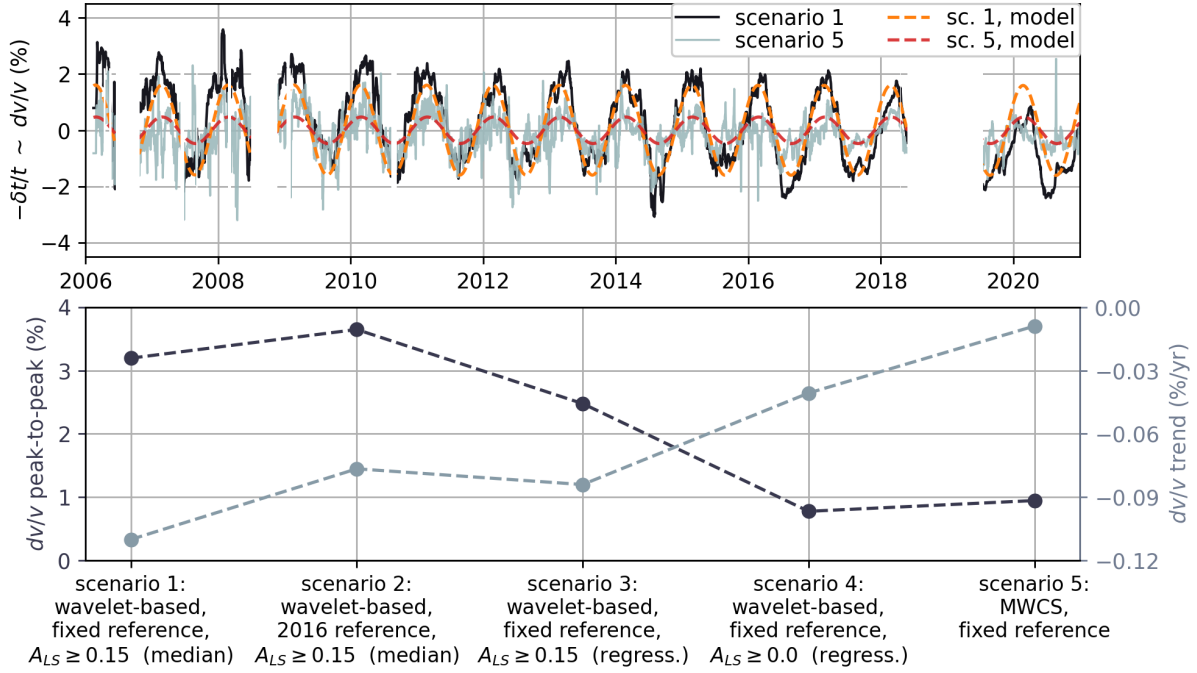
Figure S1. Comparison of different approaches to extract velocity changes from component NZ. (a) Velocity change relative to the fixed reference by calculating the median of travel time change curves associated with high 365.25 d periodicity ($A_{LS} \geq 0.15$) in each frequency bin and averaging over 2-8 Hz (black line, scenario 1; same as in Fig. 3d, main manuscript). Also shown is the velocity change relative to the fixed reference obtained from classical MWCS analysis in the frequency range 2-8 Hz (gray line, scenario 5). The orange and red dashed lines depict the velocity change model (eq. 1) fits to the two time series (scenario 1 and 5, respectively). (b) Seasonal velocity change peak-to-peak amplitude and long-term velocity change obtained by fitting the model from eq. (1) to the different velocity change time series (scenarios 1 to 5, see text for details).

Config parameter	Value
startdate	2006-01-01
enddate	2021-01-01
analysis_duration	86400
cc_sampling_rate	100.0
resampling_method	Lanczos
preprocess_lowpass	25.0
preprocess_highpass	0.01
preprocess_max_gap	10.0
preprocess_taper_length	20.0
remove_response	Y
response_format	inventory
response_prefilt	(0.005, 0.006, 30.0, 35.0)
maxlag	15.0
corr_duration	1800.0
overlap	0.0
windsorizing	3
whitening	A
whitening_type	B
stack_method	linear
cc_type	CC
components_to_compute_single_station	EN,EZ,NZ
ref_begin	2017-09-01
ref_end	2018-05-01
mov_stack	15
Filter parameter	
Low	0.1
High	25.0

Table S1. MSNoise (Lecocq et al., 2014) processing parameters used for the calculation of the single-station cross-correlations of station BW.ZUGS.